Pergamon

Tetrahedron 56 (2000) 1281–1297

TETRAHEDRON

The Conformational Analysis of 14-Membered Macrocyclic Ethers

Dean S. Clyne* and Larry Weiler†

Department of Chemistry, University of British Columbia, 2036 Main Mall, Vancouver, British Columbia, Canada V6T 1Z1

Received 3 November 1999; accepted 7 January 2000

Abstract—The conformational analysis of a series of 14-membered macrocyclic ethers possessing a variety of methyl substitution patterns was performed using both NMR spectroscopy and molecular mechanics calculations. Low temperature DNMR spectra of the macrocyclic ethers were interpreted using van der Waals steric compression and anisotropic shielding effects. The macrocyclic ether transition state energies were determined from the DNMR spectra to be approximately 9–10 kcal/mol and were compared to computer calculated values.

Introduction

The concepts of conformational analysis have been widely applied to the interpretation of chemical transformations and reaction mechanisms throughout organic chemistry. For some time we have been interested in the synthesis, conformational analysis, and reactivity of simple macrocyclic compounds with the goal of developing a conformational model to rationalize the physical and chemical properties of these compounds.[1] So far, large ring monoethers have received little attention in regards to their conformation with oxacyclooctane being the largest cyclic ether previously studied.[2] Here we report the first detailed conformational study of the 14-membered ring mono-ethers shown in Fig. 1. We were interested in the conformational preferences of these macrocyclic ethers, specifically the location of the ether oxygen, and the effect of alkyl substituents, including *gem*-dimethyl substituents, on the conformation of the ethers. We hoped to develop an increased understanding of the conformational interconversion processes of these macrocycles and of the associated transition state energies. The macrocyclic ethers of this study were prepared by the reduction of intermediate lactones obtained through the Baeyer–Villiger ring expansion of a cyclic ketone, or via the macrolactonization of a hydroxy acid.[3]

In the 1960s, Dale proposed conformations for all even membered rings ranging from 6- to 16-membered based on the diamond lattice.[4] Calculations of the enthalpies of medium and large rings were performed semi-quantitatively by Dale,[5] and subsequently with molecular mechanics methods by Anet and coworkers.[6] From these analyses, the 14-membered ring was predicted to exist largely in a quadrangular diamond lattice conformation known as the [3434] conformation by the Dale naming convention (Fig. 2).[7] There is a wealth of experimental evidence to support the [3434] conformation as the preferred conformation for

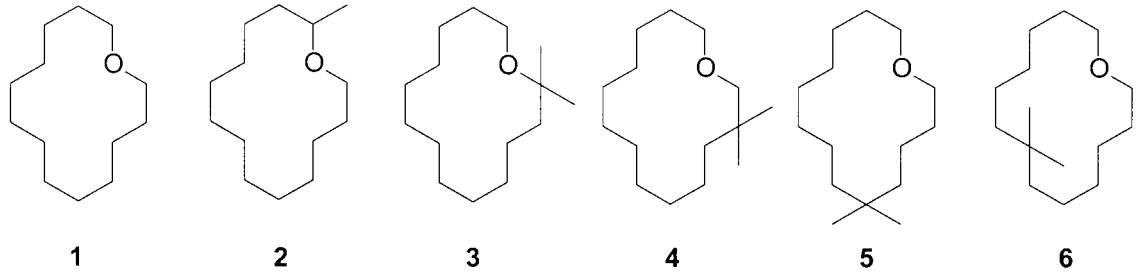

Figure 1. Macrocyclic ethers in this conformational analysis study.

Keywords: conformation; ethers; macrocyles; NMR.
* Corresponding author. Department of Chemistry, The Ohio State University, Columbus, OH 43210, USA; e-mail: dclyne@chemistry.ohio-state.edu
† Deceased 28 April 1999.

0040–4020/00/$ - see front matter
PII: S0040-4020(00)00050-8

Figure 2. The [3434] lowest energy diamond lattice conformation of cyclotetradecane.

cyclotetradecane including: X-ray crystallographic studies,[8] spectroscopy studies including NMR studies,[9] and IR and Raman studies.[10] X-ray crystallographic studies of other 14-membered macrocycles including 1,3,8,10-tetraoxacyclotetradecane,[11] cyclotetradecanone,[12] and cyclotetradecane oxime[13] have shown similar conformational preferences.

The [3434] conformation of cyclotetradecane contains four diastereotopic methylene groups, which experience varying numbers of transannular steric interactions. Dale has suggested that replacing a methylene unit of a macrocyclic ring with an ether oxygen should have a minimal perturbation on the macrocyclic system.[14] The oxygen should occupy a position in the conformation of these rings that leads to a reduction in transannular interactions. With the exception of the corner methylenes, all of the other methylenes have at least one hydrogen atom pointed into the ring. Therefore, the corner positions are predicted to be best able to accommodate geminal alkyl substitution.

Results and Discussion

NMR spectroscopy was used to analyze the conformations of these macrocyclic ethers. The introduction of the oxygen atom did offer some chemical shift dispersion in the spectra, but many of the methylene signals still overlapped, and the complete assignment of the NMR spectra was not possible. The results of low temperature DNMR experiments performed in a 4:1 mixture of $CHCl_2F$ (Freon 21) and $CHClF_2$ (Freon 22) as solvent provided information about the cyclic ether conformations, the interconversion of these conformations, and the thermodynamic barriers for these processes. Molecular mechanics calculations were used to assist the rationalization of the experimental data in an effort to more fully describe the conformational properties of the compounds studied.

The chemical shift difference of geminal protons in a molecule is influenced by a number of shielding effects including: diamagnetic anisotropy (σ_{AN}), steric compression (σ_{ST}), and electric field (σ_E). Much of the pioneering work in the determination of the diamagnetic anisotropies (σ_{AN}) of carbon–carbon and carbon–hydrogen bonds was performed by ApSimon and coworkers.[15] The steric compression effect (σ_{ST})[16] results when a hydrogen atom is rigidly held close to another atom in a molecule at a distance less than the sum of their van der Waals radii.[17] The electric field effect (σ_E) results from the polarization of carbon–carbon or carbon–hydrogen bonds by a dipole or charge. It is greatest for bonds that are parallel to each other, and of a lesser magnitude for gauche bonds or bonds of other skewed geometry.[18] As a result of these effects, the low temperature chemical shift difference between a geminal pair of axial and equatorial protons (δ_{ae}) was found to be 0.48 ppm in cyclohexane[19] and 0.50 ppm for tetrahydropyran.[20] The value of δ_{ae} was also influenced by the orientation of the carbon–oxygen bond. A study of 1,3-dioxanes showed δ_{ae} to be positive for C-2 denoting shielding of the axial proton at that position, and negative for C-5, indicating a deshielding of the axial proton at that carbon.[21]

The relative populations of these conformations were calculated from enthalpy values (ΔH°) obtained from the MM2* or MM3* calculations, and entropy values (ΔS°) with consideration of both symmetry and mixing term contributions (Eq. (1)). The rate of exchange (k_c) at coalescence can be calculated using either Eq. (2) or Eq. (3), where $\Delta\nu$ is the separation of the signals in Hertz measured at a temperature below T_c, the temperature at which the signals are broadest. Eq. (2) is applied in the case of uncoupled nuclei, and Eq. (3) is applied to cases with coupled nuclei.[22] The broadness of the signals observed in the low temperature spectra in this study prevented the measuring of J values, and the k_c values obtained here were approximated using Eq. (2). The rate of exchange was used to calculate the free energy of activation ($\Delta G_c^{\ddagger}$) for the conformational process using the Eyring equation (Eq. (4)).

$$\Delta S_{sym} = -R \ln\sigma \tag{1}$$

$$k_c = \pi\Delta\nu/2^{1/2} \tag{2}$$

$$k_c = \pi(\Delta\nu^2 - 6J^2)^{1/2}/2^{1/2} \tag{3}$$

$$\Delta G_c^{\ddagger} = RT_c \ln (k_B T_c/k_c h) \tag{4}$$

To simplify the comparison of the 14-membered macrocyclic ether conformations, an extension of the Dale nomenclature was developed to designate the position of the ether oxygen atom in the conformation. The four diastereotopic ring positions of the [3434] conformation were numbered starting with position-1 as shown below. The low energy, non-diamond lattice [3344] conformation, was numbered in a similar manner beginning with position-1 in the middle of a 4-bond side and continuing around the ring through the adjacent 3-bond side. Using this nomenclature the [3434] conformation with the ether oxygen in the middle of a 4-bond side is the [3434]-1 conformation (Fig. 3).

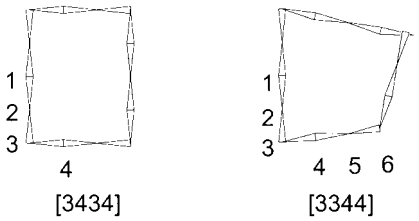

Figure 3. Naming of macrocyclic conformations.

The first ether presented here is the unsubstituted oxacyclotetradecane (**1**). At room temperature, the ^{1}H NMR spectrum of **1** in $CDCl_3$ contained a four-proton triplet at 3.41 ppm for the C-2/C-14 protons, a four-proton quintet at 1.57 ppm for the C-3/C-13 protons, a 16-proton multiplet from 1.29–1.43 ppm, and a two-proton multiplet from 1.21–1.27 ppm. The ^{13}C NMR spectrum of **1** contained seven signals with signals at 68.6 and 28.6 assigned to C-2/C-14 and C-3/C-13, respectively. The simplicity of these spectra indicates that ether **1** is undergoing rapid exchange on the NMR timescale. Each carbon resonance corresponded to a pair of methylenes in the macrocyclic ether with the exception of the signal at 23.2 ppm that was half the height of the other signals, and was assigned to C-8 on this basis.

The signal for C-4 was shielded to 23.4 ppm by both γ-gauche and van der Waals effects with the ether oxygen. A gauche geometric relationship is possible between the ether oxygen and C-4 atoms in the [3434]-1 and [3434]-4 and [3344]-1 conformations of **1**. The ether oxygen and C-4 were calculated (MM2*) to be only 2.95 Å apart, leading to a further shielding of C-4 by a van der Waals steric interaction. This shielding effect was observed in the ^{13}C spectrum and not in the ^{1}H NMR spectrum of **1** due in part to the conformational mobility of the ring at room temperature, which averaged the effect over both H-4_{exo} and H-4_{endo} (Fig. 4).

A series of low temperature DNMR experiments were performed on ether **1** (Fig. 5). The ^{1}H NMR spectrum of **1** at 220 K contained four signals of relative integration 4:4:16:2. At 200 K the high-field signal for the C-8 methylene protons was no longer visible, and at 190 K the signal for the C-3 protons had coalesced into the methylene envelope. At 180 K, the signal for the C-2/C-14 protons had broadened. Some new signals were visible downfield of the methylene envelope at 1.84 and 1.61 ppm, and also upfield of the methylene envelope at 1.04 and 0.57 ppm. At 165 K, the signal for the C-2 methylenes had split into three closely spaced signals of approximately equal intensity clustered around 3.4 ppm. The relative integration of the six signals visible in the 165 K spectrum, beginning at low field, was approximately 4:2:4:11:4:1. Further cooling to 135 K did not produce additional significant changes in the line shape of spectra of **1**.

The DNMR spectra of **1** were analyzed in terms of the conformations where the γ-gauche shielding effect of C-4 was possible. A comparison of the predicted line shapes of the H-2/H-14 and other protons in these conformations was performed by the examination of molecular models and MM2* calculations. The rationalization of the spectra began with the H-2 proton signal. This signal progressively broadened until at 165 K, it had split into three signals with chemical shifts of 3.43, 3.40 and 3.38 ppm. The relative intensity of these signals based on peak height was 1.2:1:1. As the temperature was lowered, the processes leading to ring inversion and averaging of the C-2 proton signals was slowed, and the signals for H-2_{endo} and H-2_{exo} became distinct. In the [3434]-4 conformation the corner C-2 methylene protons and the C-14 protons exist in different environments, and accordingly have different line shapes. The H-2_β proton of this conformation was deshielded as a result of the diamagnetic anisotropy of the O–C-14 bond while the H-2_α proton was deshielded by the anisotropy of the C-3–C-4 bond. These deshielding effects were predicted to be of a similar magnitude.[20] Thus, only a small $\Delta\delta$ was predicted for the C-2 protons in this conformation. The H-14_{exo} proton was deshielded by the anisotropy of the C-12–C-13 bond, and shielded by a van der Waals steric interaction between H-14_{endo} and H-11_{endo}. The magnitude of these anisotropy and steric effects were of different but similar magnitudes. The ^{1}H NMR line shape for the C-2 and C-14 methylene protons in the [3434]-4 conformation was predicted to be more complex than that observed here, and this was not considered to be a major conformation of **1** at low temperature.

In both the [3434]-1 and [3344]-1 conformations, H-2_{exo} was deshielded by the anisotropy of the C-3–C-4 bond, with a corresponding shielding of the H-2_{endo} proton. The H-2_{endo} proton was deshielded by a van der Waals steric interaction with H-5_{endo} leading to a shielding of H-2_{exo}. Here, these steric and anisotropic shielding effects were opposed, and expected to partially cancel. In the [3434]-1 conformation, a large vicinal coupling constant was expected between H-2_{endo} and H-3_β while all other coupling constants for the C-2 protons were predicted to be small. Thus, the low-field portion of the multiplet at 3.43 ppm was assigned to the H-2_{exo} proton, and the two high-field portions at 3.40 and 3.38 ppm were assigned to the H-2_{endo} proton. The slightly greater intensity of the H-2_{exo} portion of the multiplet was attributed to the presence of several small coupling constants in a complex pattern, and to the broadened line shape at low temperature.

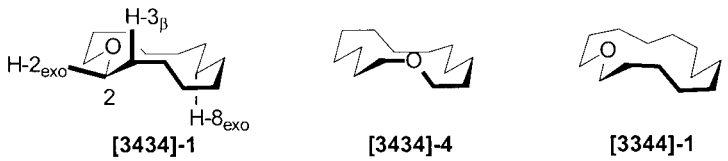

Figure 4. Possible low energy conformations of **1**.

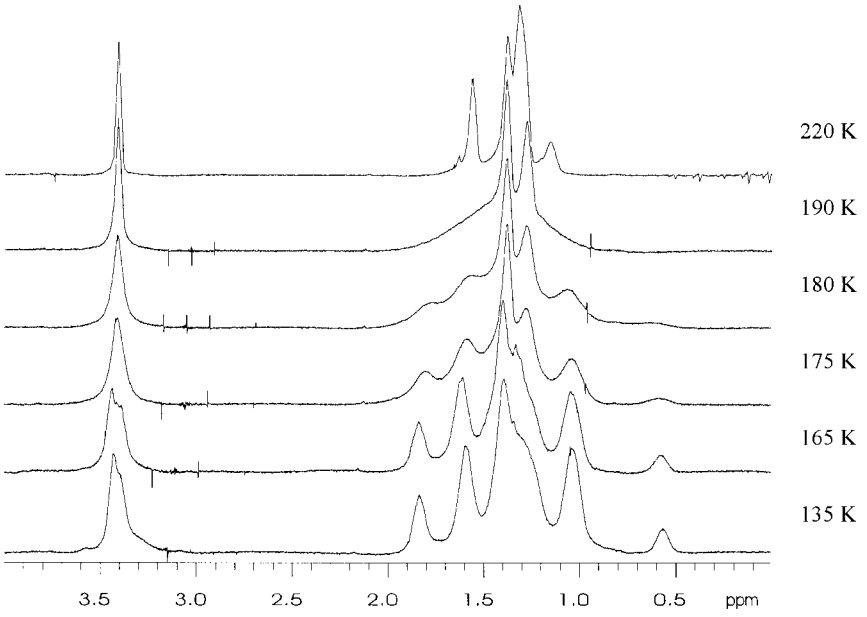

Figure 5. Variable temperature ^{1}H NMR (500 MHz) of ether **1**.

In the low temperature spectra, the high-field signal at 0.57 ppm, of relative intensity 1:4 in comparison to the signals of the C-2/C-14 protons at 3.4 ppm, was assigned to H-8_{exo} on the basis of the following rationalization. In the [3434]-1 conformation, the H-8_{endo} proton was deshielded by van der Waals steric interactions with the H-5_{endo}/H-11_{endo} protons, leading to a shielding of the H-8_{exo} proton. No transannular steric repulsion between H-8_{endo} and the ether oxygen appeared possible based on the 3.10 Å calculated distance (MM2*) between these atoms.[17] The H-8_{exo} proton was further shielded by electric field effects caused by the parallel bonds of the C-6_α and C-10_α protons. The sum of these effects causes an upfield shift of the H-8_{exo} proton signal. The H-8_{endo} proton signal was believed to be overlapped by the methylene envelope at low temperature. There are no protons in the [3344]-1 conformation capable of this upfield signal since the distorted geometry of this conformation does not allow for an alignment of these shielding effects. The low temperature spectra of **1** were concluded to be consistent with the [3434]-1 conformation in which both ring inversion and pseudorotation have slowed.

The C-3/C-13 corner protons of the [3434]-1 conformation of **1** could also be assigned in the low temperature spectra. The C-3_β proton was deshielded by the diamagnetic anisotropy of the C-4–C-5 and O–C-2 bonds. These effects reinforce each other to give a large $\Delta\delta$ with a chemical shift of 1.84 ppm for the H-3_β/H-13_β protons and 1.61 ppm for the H-3_α/H-13_α protons. The upfield signal of the H-3_α/H-13_α protons was overlapped with that of two other unidentified protons. The signals of the remaining protons of **1** were overlapped between 1.0–1.5 ppm, and could not be unambiguously assigned.

A molecular mechanics search using the Monte Carlo technique and the MM2* force field revealed the global minimum conformation of **1** to be the [3434]-1 conformation **1a** with the [3344]-1 conformation **1b** calculated to have the next lowest energy, 0.99 kcal/mol higher (Fig. 6). These calculations suggested the existence of three other low energy conformations **1c**–**1e** within 2 kcal/mol of the global minimum conformation. Higher energy conformations were ignored as they were not considered to be significantly populated over the temperature range studied. The relative populations of these conformations at 135 K were calculated from enthalpy values ($\Delta H°$) obtained from the MM2* calculations, and entropy values ($\Delta S°$). The [3434]-1 conformation of **1** was calculated to be the major conformation (93%) in agreement with the DNMR data.

The transition state energies for the interconversion of conformations of **1** were determined from the DNMR spectra. The $\Delta\nu$ for the C-2 protons was 20 Hz at low

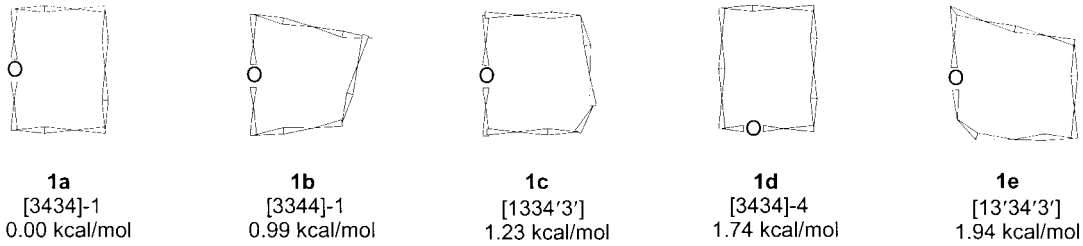

Figure 6. MM2* calculated low energy conformations of **1**.

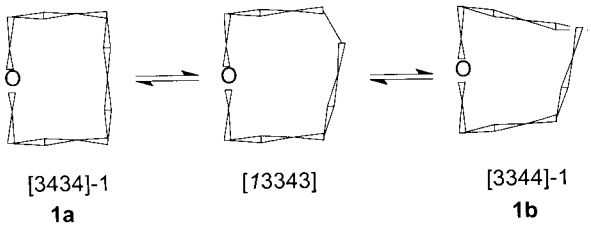

Figure 7. Single corner movement transition state for interconversion of conformations **1a** and **1b**.

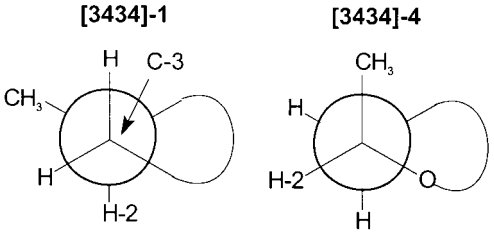

Figure 8. Newman projections of **2** showing the geometry of C-2 in the [3434]-1 and [3434]-4 conformations.

temperature with a T_c of 170 K and the C-3 protons had a $\Delta\nu$ of 110 Hz with a T_c of 190 K. This corresponded to a $\Delta G^{\ddagger}$ of 8.7±0.2 kcal/mol. This is similar in magnitude to transition state energies calculated for cyclotetradecane obtained via ^{1}H and ^{13}C DNMR studies ($\Delta G^{\ddagger}$=7 kcal/mol, T_c=158 K).[23]

A mechanism proposed by Dale for the interconversion of cyclic conformations involves the movement of a single corner atom within the ring.[24] This process can result in the exchange of both ring atoms and ring substituent sites. The most favorable transition state was proposed to have a 0° torsional angle between the new and the old corner atoms, which become eclipsed during the interconversion process. The *syn* eclipsed bond of this transition state is considered to be a one-bond side. This is written in italics to differentiate the transition state structure from that of conformational minima. The [*1*3343] barrier between the [3434] and [3344] conformations of cyclotetradecane was calculated by Dale using semi-quantitative methods to be 13.8 kcal/mol.[24] In comparison to the hydrocarbon many transition state structures are made possible for the ether by the introduction of the oxygen atom. The energies of all possible transition states of **1** were not determined here. The energy of the [*1*3343] transition state structure for the interconversion of the [3434]-1 and [3344]-1 conformations **1a** and **1b** by the Dale mechanism was calculated with the dihedral drive method[25] using 10° increments of the appropriate dihedral angles to be 12.9 kcal/mol (Fig. 7).

The room temperature ^{1}H NMR spectrum in $CDCl_3$ of the C-2 methyl substituted ether **2** contained a one-proton doublet of triplets at 3.61 ppm for one of the C-14 protons, a one-proton doublet of doublet of quartets at 3.43 ppm for the C-2 proton, a one-proton doublet of doublet of doublets at 3.22 ppm for the other C-14 proton, a 22-proton multiplet from 1.10–1.73 ppm, and a three-proton doublet at 1.09 ppm for the C-15 methyl protons. The three low-field signals were unambiguously assigned with ^{1}HCOSY and NOE spectra. Irradiation of the H-14 signal at 3.22 ppm showed an enhancement of both the geminal H-14 signal and the *syn* H-2 signal at 3.43 ppm. The ^{13}C NMR spectrum of **2** contained 14 lines, two of which were at low-field at 73.3 and 66.0 ppm, and these were assigned to the C-2 and C-14 carbons, respectively. The highest field carbon at 19.8 ppm was assigned to the C-15 methyl group. The signal for C-12 was shielded to 23.0 ppm as a result of the γ-gauche effect. Unfortunately, due to the overlap of signals in the ^{1}H NMR spectrum, and the small $\Delta\delta$ between several signals in the ^{13}C NMR spectrum, not all of the remaining signals could be assigned.

Examination of the coupling constants for the H-2 and H-14 protons provided some information about the preferred conformation of this macrocyclic ether. The H-2 proton had large and small coupling constants to the adjacent methylene protons (Table 1). In the [3434]-1 conformation the C-15 methyl group would be exo and the H-2 proton endo to the ring, with both large and small coupling constants predicted between H-2 and the protons at C-3 (Fig. 8). In the [3434]-4 conformation, the C-15 methyl group occupies a corner position. Since a carbon–oxygen bond is shorter than a carbon–carbon bond, a C-15$_\beta$ methyl group is preferred over a C-15$_\alpha$ methyl group as the 1,3-interaction would be greater between a C-15$_\alpha$ methyl group and H-14$_{exo}$. In this conformation, no large coupling constants were expected between H-2 and the C-3 protons (Figs. 8 and 9).

The coupling constants for the H-2 and H-14 protons in the [3434]-1, [3434]-4, and [3344]-1 conformations of **2** were calculated and compared to the actual values (Table 1). The calculated coupling constants for H-2 in the [3434]-4 conformation and H-14$_{exo}$ in the [3344]-1 conformation with C-14 adjacent to a 4-bond side were in poor agreement with the observed values. These conformations were not predicted to be major conformations of **2** and were not considered further.

In the DNMR spectrum of **2** at 220 K the signals had broadened (Fig. 10). At 190 K the signals had broadened

Table 1. Experimental and calculated coupling constants (*J*) for the low energy conformations of **2**

Proton	Experimental (Hz)	Calculated (Hz) conformations				
		Boltzmann[a]	[3434]-1	[3434]-4	[3344]-1	[3344]-1
H-2	3.1 9.2	3.6 8.5	1.9 11.6	1.7 5.0	1.9 11.5	3.1 11.6
H-14$_{endo}$	3.0 10.6	2.3 10.7	1.7 11.9	2.4 11.9	3.1 11.8	1.5 11.8
H-14$_{exo}$	4.2 4.2	3.0 4.0	2.2 3.8	1.5 4.7	1.0 5.6	2.4 3.6

[a] Calculated coupling constants were averaged for a Boltzmann distribution weighted set of conformations.

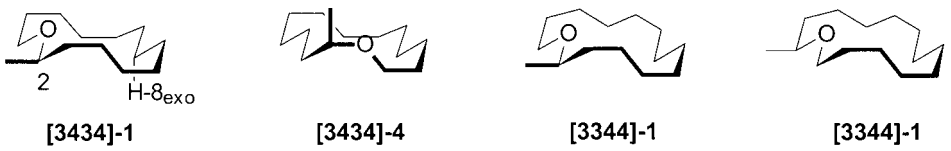

Figure 9. Possible low energy conformations of **2**.

further, and a small signal at 0.57 ppm became visible upfield of the C-15 methyl signal. The relative intensity of this upfield signal increased as the temperature was lowered. At 180 K, the low-field signals of the C-2 and C-14 protons were broadest. At 170 K the line shape of these signals changed with additional minor signals becoming visible at the feet of the originals indicative of the freezing out of unequally populated conformations. Further cooling to 130 K did not produce additional significant changes in the line shape of spectra of **2**.

The additional small signals present in the low-field portion of the spectra at 3.71, 3.34 and 3.03 ppm belong to minor conformation(s) of **2**. The similarity of the chemical shifts of the major low-field signals at both room temperature and low temperature suggested that the major conformation was the same at both temperatures. Additional small signals were expected between 1.5 and 2.0 ppm for minor conformations, but no such signals were observed. Presumably, these were concealed by the proton signals of the major conformation visible in that region. Examination of the low temperature spectra in the region of the C-15 methyl group signal at 1.03 ppm showed other signals at 0.90 and 1.16 ppm. The relative integration of the 0.90 ppm signal to the 3.34 and 3.03 ppm minor signals was approximately 1:3.4 but whether this upfield signal could be assigned to a C-15 methyl group of a minor conformation, or to other major conformation proton signals was unclear.

The signal at 0.57 ppm in the low temperature spectra of **2**, was similar to the high-field signal observed in the DNMR study of ether **1**. The relative integration of this high-field signal and the signal at 3.12 ppm for H-14_{exo} of the major conformation was approximately 1:1. The geometry of the C-8 protons in the [3434]-1 conformation of ethers **1** and **2** were expected to be similar. Here, the H-8_{endo} proton would be deshielded by steric interactions with H-5_{endo} and H-11_{endo} calculated to be 2.22 Å from H-8_{endo}. This would lead to a shielding of H-8_{exo}, and an upfield shift of this proton signal to 0.57 ppm in the low temperature spectra of **2**. The geometry of the [3434]-4 conformation would lead to two high-field signals in the low temperature spectra, while the skewed geometry of the [3344]-1 conformation was not predicted to produce the large shielding of any protons. The [3434]-1 conformation was therefore believed to be the major conformation of **2**. In this conformation, the $\Delta\delta$ between the H-14_{endo} and H-14_{exo} protons can be explained by a deshielding of the H-14_{exo} proton by the diamagnetic anisotropy of the C-12/C-13 carbon–carbon bond.

A molecular mechanics search for the lowest energy conformations of **2** was conducted using the Monte Carlo technique and the MM2* force field. These calculations gave a total of 13 conformations within 2 kcal/mol of the global minimum conformation, the [3434]-1 conformation **2a** (Fig. 11). The second lowest energy conformation was the [3434]-4 conformation **2b** with the methyl substituent at a corner position. The relative populations of these conformations at 135 K were calculated to be **2a** (73%) and **2b**–**2d** (<10% each) from relative energy values obtained from the MM2* calculations.

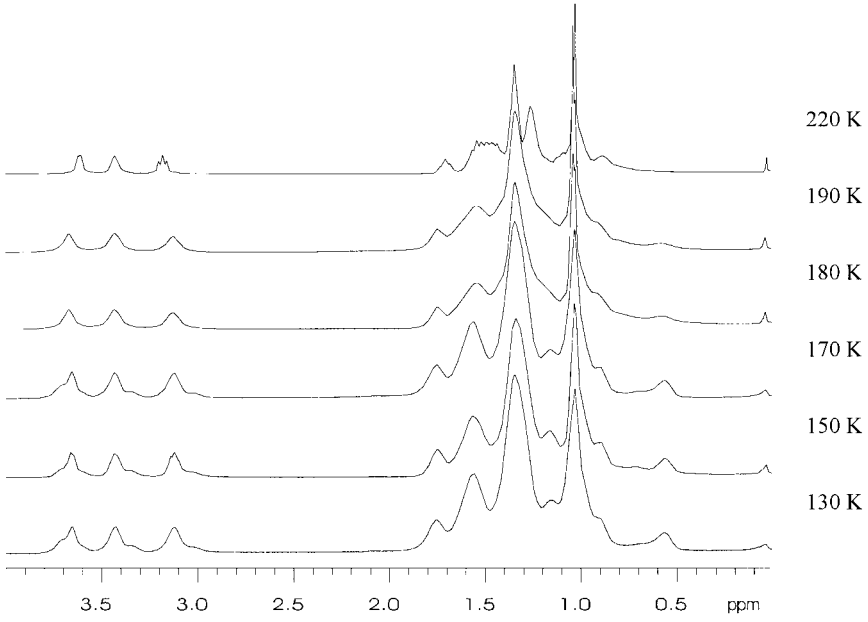

Figure 10. Variable temperature ^{1}H NMR (500 MHz) of ether **2**.

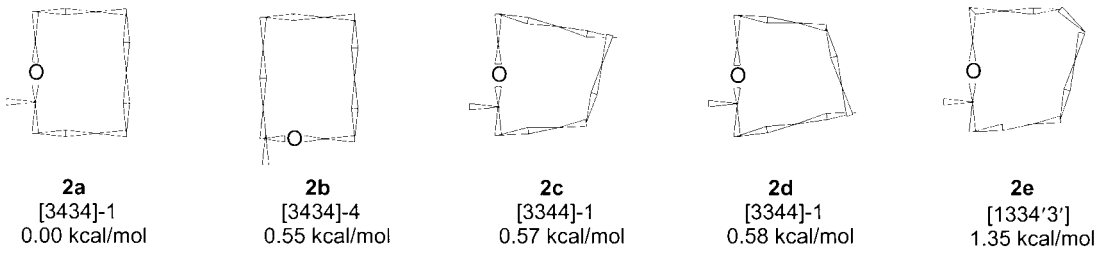

Figure 11. MM2* calculated low energy conformations of **2**.

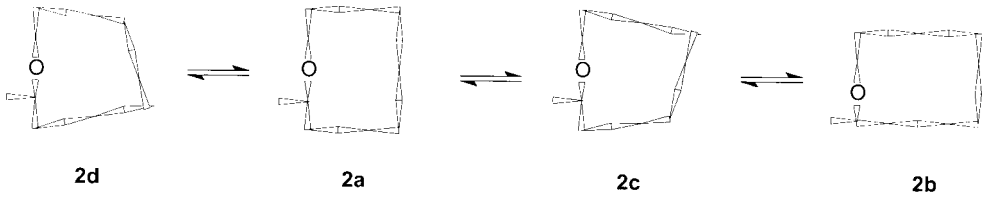

Figure 12. Interconversion of conformations of **2** via single corner movements.

The DNMR study indicated unequally populated conformations of **2** to be present at low temperature. The MM2* calculations of **2** were in agreement, with three conformations of approximately equal energy found within 0.6 kcal/mol of the global minimum. The low-field major and minor signals had relative integrations of approximately 2.8:1 at 150 K. This corresponded to a 74:26 ratio of conformations, and an energy difference of 0.31 kcal/mol in reasonable agreement with the values obtained from the MM2* calculations.

The transition state energy for the interconversion of conformations of **2** were calculated from the DNMR spectra to be 8.8±0.1 kcal/mol from the low-field signals with $\Delta\nu$ values of approximately 39 Hz and a T_c of 180 K. Conformation **2a** can interconvert via the Dale single corner movement mechanism[26] with the low energy conformations **2c** and **2d** via related [*1*3343] transition state structures (Fig. 12). The energies of these structures were calculated with the dihedral drive method[25] to be 13.0 and 12.8 kcal/mol, respectively. The energy of the transition state structure for the interconversion of conformations **2c** with **2b** was calculated to be 9.8 kcal/mol.

The room temperature ^{1}H NMR spectrum in $CDCl_3$ of ether **3**, a C-2 *gem*-dimethyl substituted ether contained a two-proton triplet at 3.25 ppm for the C-14 protons, a two-proton quintet at 1.57 ppm for the C-13 protons, a six-proton singlet at 1.13 ppm for the C-2 methyl groups, and a 20-proton multiplet from 1.23–1.43 ppm for the remaining proton signals. The ^{13}C spectrum of this compound contained 14 lines. Low-field signals at 73.9 and 58.9 ppm were assigned to the quaternary C-2 and C-14 methylene carbons. A signal at 38.0 ppm was assigned to C-3 and the geminal methyl carbons C-15 and C-16 were assigned to the signal at 26.7 ppm (Fig. 13).

The ^{1}H NMR spectrum of **3** at 220 K contained four broad signals (Fig. 14). As the temperature was lowered, the downfield signal at 3.25 ppm for the C-14 protons split to give a pair of signals at 3.31 and 3.15 ppm (T_c=180 K). The signal for the C-13 protons at 1.57 ppm also broadened and split as the temperature was lowered to give signals at 1.69 and 1.50 ppm. The signal for the geminal methyl groups at 1.13 ppm split at temperatures lower than 190 K to give signals at 1.15 and 1.10 ppm. Two signals at 0.93 and 0.67 ppm were also visible in the high-field region of the low temperature spectra. The observation of one set of major signals for the geminal methyl groups led to the prediction of a single conformation predominating at low temperature.

The [3434]-1 conformation would be highly disfavored in the case of ether **3** as the C-2 *gem*-dimethyl group would be at a non-corner position in this conformation. Two possible diamond lattice conformations with C-2 at a corner position were the [3434]-4 and [3434]-2 conformations, and both of these were considered as possible conformations of **3** in the analysis of the DNMR data. In the [3434]-2 conformation, C-14 was located in the middle of a 4-bond side of the ring. In this conformation, H-14$_{exo}$ was shielded by van der Waals interactions between the H-14$_{endo}$ proton, and the H-3$_{endo}$ and H-11$_{endo}$ protons calculated to be 2.10 and 2.14 Å, respectively, from H-14$_{endo}$. The H-14$_{exo}$ proton was further shielded by electric field effects caused by the parallel alignment of the carbon–hydrogen bonds between C-14 and H-14$_{exo}$, and C-12 and H-12$_{\beta}$. The reinforcement of these shielding effects would result in a larger $\Delta\delta$ than observed here in the low temperature spectra of **3**. Moreover, in the [3434]-2 conformation, a pair of large coupling constants (^3J, J_{gem}) were expected for BOTH the H-14$_{endo}$ and H-14$_{exo}$ protons. The predicted line shape for the H-14 protons in the [3434]-2 conformation was in poor agreement with that

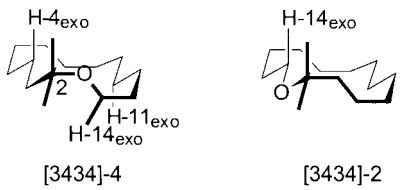

Figure 13. Possible low energy conformations of **3**.

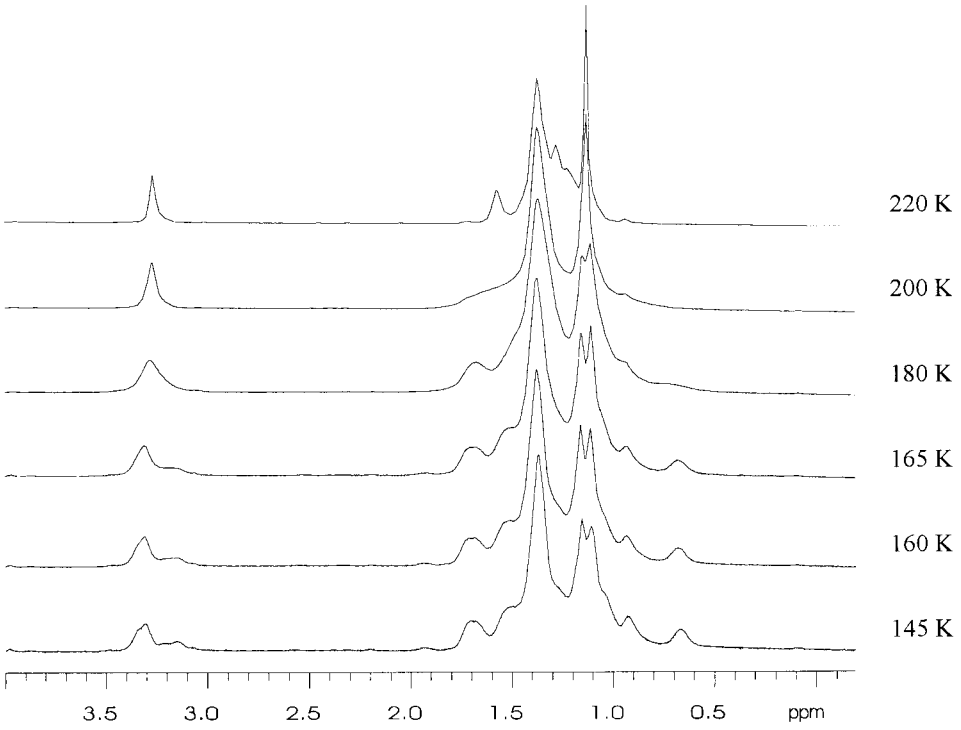

Figure 14. Variable temperature ^{1}H NMR (500 MHz) of ether **3**.

observed here, and this conformation was not considered further.

In the [3434]-4 conformation, the H-14$_{endo}$ proton was shielded by the diamagnetic anisotropy of the C-12–C-13 bond, and deshielded by van der Waals steric interactions with the H-11$_{endo}$ and H-3$_{endo}$ protons, calculated to be 2.20 and 2.17 Å away from H-14$_{endo}$. Conversely, the H-14$_{exo}$ proton was deshielded by the anisotropy of the neighboring bond, and shielded by the van der Waals interactions. The relative magnitudes of these effects were unknown, but the anisotropy contribution was thought to be larger. The H-14$_{endo}$ proton was expected to have two large coupling constants, a vicinal coupling to H-13$_{\beta}$, and a geminal coupling to H-14$_{exo}$. In contrast, H-14$_{exo}$ would have only the large J_{gem} coupling constant. On the basis of these chemical shift and coupling constant arguments, the broad signal at 3.15 ppm was assigned to H-14$_{endo}$, and the sharper signal at 3.31 ppm to the H-14$_{exo}$ proton.

In the room temperature ^{1}H NMR spectrum of **3**, the C-13 protons β to the ether oxygen, were resolved from the methylene envelope while the C-3 protons were overlapped by the methylene envelope. However, at low temperature, two signals were visible at 1.69 and 1.50 ppm, which were assigned to the four protons β to the ether oxygen. In the [3434]-4 conformation, H-3$_{endo}$ was deshielded by the diamagnetic anisotropy of the O–C-2 bond, and also by the carbon–carbon bond between C-2 and the β-methyl group. A van der Waals steric interaction with H-14$_{endo}$ further deshields this proton. The H-13$_{\alpha}$ proton was shielded by the anisotropy of both the C-14–O bond, and the C-11–C-12 bond. No van der Waals steric interactions were expected for the C-13 corner protons in the [3434]-4 conformation since both were exo to the ring. The combination of these effects lead to the assignment of the lower field signal at 1.69 ppm to the H-3$_{endo}$ and H-13$_{\beta}$ protons, and the higher field signal at 1.50 ppm to the more shielded H-3$_{exo}$ and H-13$_{\alpha}$ protons. The interconversion of the C-2 geminal methyl group signals of **3** was slowed at low temperature, and a pair of signals of approximately equal intensity at 1.15 and 1.10 ppm was visible. The unambiguous assignment of these signals to the C-2$_{\alpha}$ and C-2$_{\beta}$ methyl groups was not possible.

The high field signals in the DNMR spectra of **3** were assigned to the H-4$_{exo}$ and H-11$_{exo}$ protons. In the [3434]-4 conformation, the H-4$_{endo}$ and H-11$_{endo}$ protons were deshielded as a result of a series of van der Waals steric interactions with the H-7$_{endo}$, H-11$_{endo}$, H-14$_{endo}$, and H-8$_{endo}$ protons. These effects result in the shielding of the H-4$_{exo}$ and H-11$_{exo}$ protons. An additional van der Waals interaction between the ether oxygen and H-4$_{endo}$, calculated to be 2.60 Å away, further shields H-4$_{exo}$.[17] The higher field signal at 0.67 ppm was therefore assigned to H-4$_{exo}$, and the other signal at 0.93 ppm to the H-11$_{exo}$ proton.

A molecular mechanics search (MM3*) for the lowest energy conformations of **3** was conducted using the Monte Carlo technique. These calculations gave a total of eight conformations within 2 kcal/mol of the calculated lowest energy conformation, the [3434]-4 conformation **3a** (Fig. 15). The second lowest energy conformation was the [3434]-2 conformation **3b**. As expected, the *gem*-dimethyl group was situated at a corner position in all of the low energy conformations. The relative population of these conformations at 145 K was calculated from the MM3* strain energies, and the [3434]-4 conformation **3a** was the major conformation (91%) in agreement with the DNMR data.

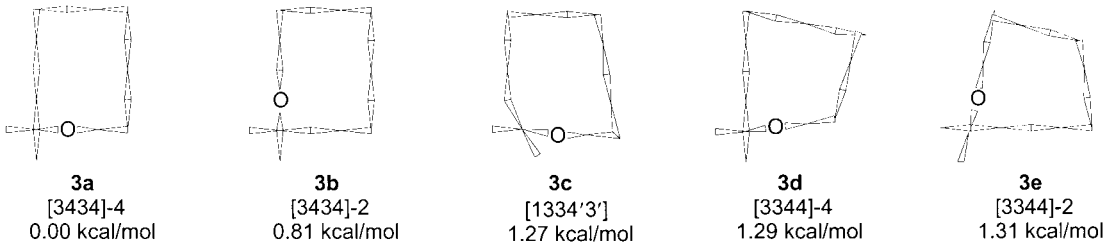

Figure 15. MM3* calculated low energy conformations of **3**.

The transition state energies for the interconversion of conformations of **3** were determined from the DNMR spectra. The $\Delta\nu$ for the β-proton signals was 95 Hz with a T_c of 200 K, while the $\Delta\nu$ for the geminal methyl signals was 26 Hz with a T_c of 190 K corresponding to a $\Delta G^{\ddagger}$ of 9.1 ± 0.4 kcal/mol. This value is higher than that obtained for the unsubstituted oxacyclotetradecane (**1**). The energies of the Dale interconversion mechanism transition states were estimated (MM3*) with the dihedral drive method.[25] An incremental step of 10° was used in this calculation. The energies of the [*1*3343] transition state conformations for the interconversion of conformation **3a** with the **3e** and **3d** conformations were calculated to be 13.3 and 12.8 kcal/mol (Fig. 16). The energy of the transition state conformation involved in the interconversion of the higher energy **3b** and **3e** conformations was calculated to be 13.5 kcal/mol.

The next macrocyclic ether examined was **4** with a *gem*-dimethyl group located at C-3, β to the ether oxygen. The room temperature ^{1}H NMR spectrum in $CDCl_3$ of this ether contained a two-proton triplet at 3.38 ppm for the C-14 protons, a two-proton singlet at 3.03 ppm for the C-2 protons, an 18-proton multiplet between 1.18–1.42 ppm, and a six-proton singlet at 0.84 ppm for the C-3 geminal methyl groups. Data from a ^{1}H COSY experiment was used to assign the signal at 1.55 ppm to the C-13 protons. The ^{13}C spectrum of **4** contained 14 lines, and the two lowest field signals at 77.4 and 68.8 ppm were assigned to C-2 and C-14, respectively. The signal at 34.1 ppm was assigned to the C-3 quaternary carbon, and the signal at 37.4 ppm to C-4, the adjacent methylene. The chemical shift of the C-3 geminal methyl groups was 26.1 ppm (Fig. 17).

In DNMR experiments of **4**, the C-2 and C-14 methylene signals were broad at 200 K (Fig. 18). At this same temperature, the signal for the C-13 protons was unresolved on the low-field shoulder of the methylene envelope, and the C-3 geminal methyl signal was also broad. In the upfield portion of the spectrum at 190 K, the C-3 geminal methyl signal had split into a pair of equally intense signals at 0.93 and 0.77 ppm. At lower temperatures, the line shape of the α-proton signals became distinct with a total of seven peaks visible at 140 K in the region between 2.5 and 3.7 ppm, indicative of the presence of multiple conformations. Three signals were visible at 1.61, 1.75 and 1.84 ppm in the region where the C-13 proton signals were expected. The geminal methyl signals were quite broad, but no additional peaks were visible in that region to suggest the presence of minor conformations. At temperatures below 175 K an unresolved, broad peak at 0.62 ppm on the high-field shoulder of the methyl signals was also visible.

Low energy conformations of **4** were expected to have the C-3 *gem*-dimethyl substituted carbon at a corner position of the ring. This configuration would allow for the ether oxygen to be located in the middle of a 4-bond side in the [3434]-1 conformation, or on the 3-bond side in the [3434]-4 conformation. Non-diamond lattice [3344]-1 conformations of **4** with the *gem*-dimethyl group at a corner position flanked by either two 4-bond sides, or a 3-and a 4-bond side were also expected to have low strain energy. These conformations were considered first in the analysis of the DNMR spectra of **4**.

The downfield portion of the low temperature spectra of **4**

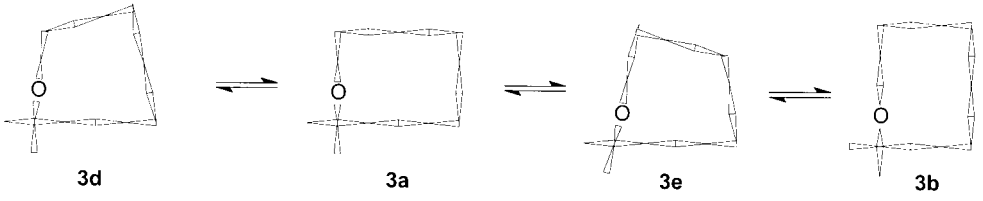

Figure 16. Interconversion of conformations of **3** via single corner movements.

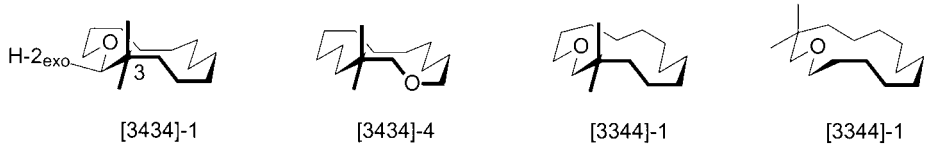

Figure 17. Possible low energy conformations of **4**.

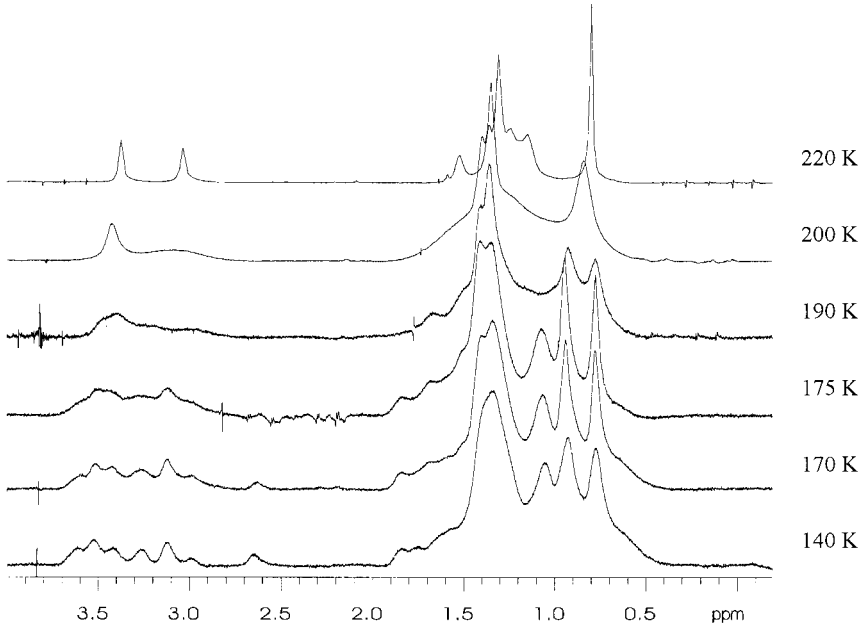

Figure 18. Variable temperature ^{1}H NMR (500 MHz) of ether **4**.

contained seven peaks. Although the three lowest field peaks appeared in a triplet-like pattern, the $\Delta\delta$ values for these peaks were approximately 50 Hz, and therefore too large to have been the result of vicinal coupling. The downfield peaks of the DNMR spectra at low temperature therefore resulted from a number of conformations. The four higher field signals at 3.27, 3.12, 2.99 and 2.65 ppm were assigned to the C-2 protons of **4**. The downfield, more intense pair of signals in this group was assigned to the major conformation and the upfield pair of signals to a minor conformation. The approximate relative intensities of these signals were 2.2:1 corresponding to an energy difference between the major and minor conformations of 0.21 kcal/mol. The predicted $\Delta\delta$ values for the C-2 protons in the conformations suggested above were compared in an effort to identify these major and minor conformations of **4**, with small and large $\Delta\delta$ values, respectively.

In the [3434]-1 conformation, the H-2_{exo} proton was deshielded by the anisotropy of the C-3–C-4 bond, and shielded by the anisotropy of the carbon–carbon bond between C-3 and the C-3_{β} methyl group. This proton was also shielded by a van der Waals steric interaction between the H-2_{endo} and H-5_{endo} protons. These effects predict a small $\Delta\delta$ for the C-2 protons in this conformation with the H-2_{exo} proton at higher field. In the [3434]-4 conformation, the H-2_{exo} proton was deshielded by the anisotropy of the C-3–C-4 bond, but shielded by the anisotropy of the carbon–carbon bond between C-3 and the C-3_{α} methyl group. This proton was further shielded by van der Waals steric interactions between the H-2_{endo} proton and the H-5_{endo} and H-13_{endo} protons calculated to be 2.20 and 2.19 Å from H-2_{endo}. The predicted combination of these effects was a large $\Delta\delta$ value for the C-2 protons in this conformation with the H-2_{exo} proton at higher field. In the [3344]-1 conformation with the *gem*-dimethyl substituted corner atom flanked by a pair of 4-bond sides, the H-2_{exo} proton was deshielded by the anisotropy of the C-3–C-4 bond, but shielded by the anisotropy of the carbon–carbon bond between C-3 and the C-3_{β} methyl group. The magnitude of these effects was unequal as a result of the distorted geometry of this non-diamond lattice conformation. The H-2_{exo} proton was also shielded by a van der Waals steric interaction between the H-2_{endo} and H-5_{endo} protons calculated to be 2.27 Å apart. A large $\Delta\delta$ value was predicted for the C-2 protons in this conformation as a result of these effects. In the other [3344]-1 conformation where the substituted corner atom was between a 3- and a 4-bond side, the environment of the C-2 protons was similar to that of the C-2 protons in the [3434]-1 conformation, and a small $\Delta\delta$ value was predicted.

In summary, the chemical shift differences between the C-2 protons is small in the [3434]-1 conformation and the [3344]-1 conformation with the *gem*-disubstituted corner atom flanked by a 3- and a 4-bond side making these possible candidates for the major conformation of **4**. The $\Delta\delta$ value of the C-2 protons was predicted to be large for the [3434]-4 and the [3344]-1 conformation where a pair of 4-bond sides flanked the *gem*-disubstituted corner atom. These were possible candidates for the minor conformation of **4**.

A similar analysis was performed for the three signals of the C-14 protons at 3.61, 3.53 and 3.42 ppm where the triplet-like pattern was the result of overlapping unequally intense doublets. The two signals for the minor conformation were the peaks at 3.61 and 3.53 ppm, with the major conformation signals appearing at 3.42 and 3.53 ppm. The observed $\Delta\delta$ values of the C-14 protons in the DNMR spectra for both the major and minor conformations of **4** were small. A comparison of the shielding effects experienced by the C-14 protons in the four suggested low energy conformations predicted in all cases small $\Delta\delta$ values, and this analysis did not assist in further identifying the major and minor conformations.

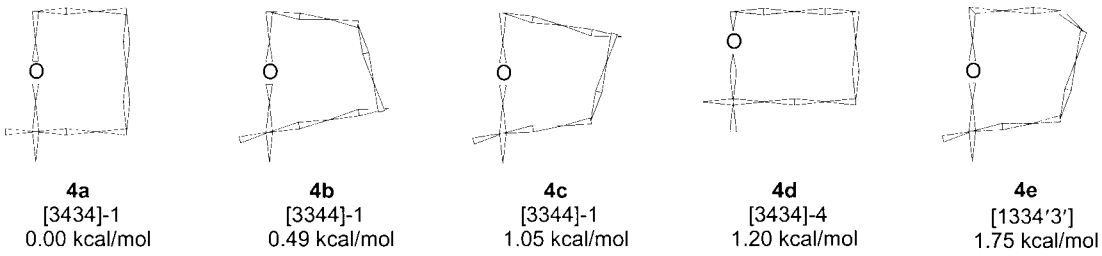

Figure 19. MM3* calculated low energy conformations of **4**.

The signal of the C-3 *gem*-dimethyl groups of **4** split as the temperature was lowered to give a pair of signals at 0.93 and 0.77 ppm. Unfortunately, no signals for the methyl groups of the minor conformation could be identified. These signals may have been hidden by the broad signals of the major conformation methyl groups or by other proton signals in this region.

A molecular mechanics search for low energy conformations of **4** was conducted with the MM3* force field using the Monte Carlo technique. The calculated global minimum was the [3434]-1 conformation **4a** with the [3344]-1 conformation **4b** calculated to have the next lowest energy, 0.49 kcal/mol higher. These calculations suggested the existence of five other conformations within 2 kcal/mol of the global minimum conformation (Fig. 19). The relative population of these conformations at 140 K were calculated from the MM3* strain energies and **4a** was the major conformation (81%) with the second most populated conformation, **4b**, also significantly populated (14%). These calculations were consistent with the DNMR data and above proposals. The calculated relative energies of the major and minor conformations **4a** and **4b** was 0.49 kcal/mol, in agreement with the 0.21 kcal/mol energy difference obtained from the DNMR spectra.

At low temperature, the $\Delta\nu$ of the C-3_α and C-3_β methyl signals was 76 Hz with a T_c of 195 K. The signals of the C-14 protons had $\Delta\nu$ values of approximately 48 Hz in the major and minor conformations, respectively, and a T_c of 195 K while the $\Delta\nu$ values for the C-2 protons were 72 and 172 Hz in the major and minor conformations with a T_c of approximately 200 K. This corresponded to a $\Delta G^{\ddagger}$ of 9.4 ± 0.1 kcal/mol. The energies of the Dale [*13*343] transition states for the interconversion of the global minimum [3434]-1 conformation **4a** with the **4b** and **4c** conformations were calculated using the dihedral drive method to be 10.2 and 9.4 kcal/mol, respectively (Fig. 20). The energy of the transition state conformations needed to complete the cycle through the [3434]-4 conformation **4d** were calculated to be 9.5 kcal/mol above the global minimum from **4b**, and 10.5 kcal/mol from **4c**. These values were in good agreement with the experimental transition state energies derived from the NMR data.

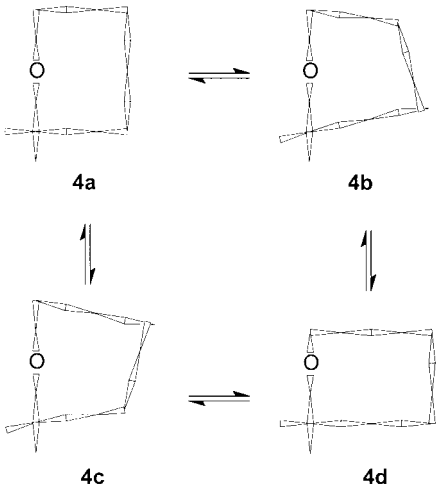

Figure 20. Interconversion of conformations of **4** via single corner movements.

The next macrocyclic ethers examined had *gem*-dimethyl groups remote from the ether oxygen. The first of these was ether **5** with a *gem*-dimethyl group at C-6. The room temperature ^{1}H NMR spectrum of **5** in $CDCl_3$ contained a two-proton triplet at 3.43 ppm for the C-2 protons, a two-proton triplet at 3.42 ppm for the C-14 protons, a two-proton quintet at 1.60 ppm for the C-13 protons, a two-proton triplet at 1.54 ppm for the C-3 protons, a ten-proton multiplet from 1.29–1.42 ppm, a six-proton multiplet between 1.11–1.17 ppm, and a six-proton singlet at 0.84 ppm for the C-6 geminal methyl groups. The long-range ^{1}H–^{13}C NMR data was integral in distinguishing the signals in the C-2 and C-14 regions of the macrocycle. The assignment of the C-2 to C-4 and the C-14 to C-12 portions of the macrocyclic ether were made possible by a correlation between a carbon adjacent to the quaternary C-6 and a proton of a methylene γ to the ether oxygen. The ^{13}C NMR spectrum contained 14 lines. Downfield signals at 68.2 and 67.7 ppm were assigned to C-2 and C-14. The chemical shifts of C-5, C-7 and the quaternary carbon, C-6, were 37.8, 38.9 and 32.4 ppm, respectively (Fig. 21).

The ^{1}H NMR spectrum of **5** at 220 K had already broadened in comparison to the room temperature spectrum (Fig. 22). The signals of the α-methylenes, C-2 and C-14, at 3.4 ppm broadened further at lower temperatures with a T_c of 190 K. Below this temperature, two closely spaced signals were

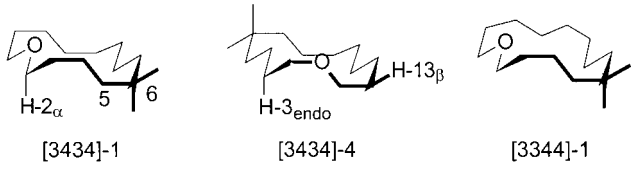

Figure 21. Possible low energy conformations of **5**.

visible at 3.46 and 3.42 ppm. No minor signals indicative of minor conformations were visible in this region, suggesting the presence of only a single conformation at low temperature. The β-proton signals between 1.5 and 1.6 ppm in the room temperature spectrum had already coalesced above 220 K, the highest temperature of this DNMR series. At lower temperatures, signals at 1.86, 1.59 and 1.52 ppm were visible for these protons. The signal for the C-6 geminal methyl groups at 0.84 ppm did broaden somewhat as the temperature was lowered, but these protons remained averaged over the temperature range examined. A detailed analysis of the remaining proton signals in **5** was not possible due to signal overlap.

Generally, the diamond lattice [3434] conformations of 14-membered rings are preferred over non-diamond lattice [3344] conformations. Conformations with the ether oxygen in the middle of a 4-bond side, and the *gem*-dimethyl group at a corner position are also preferred. The combination of these factors suggested some likely low energy conformations of **5** including the diamond lattice [3434]-1 and [3434]-4 conformations, and the non-diamond lattice [3344]-1 conformation. These conformations received primary consideration in the analysis of the DNMR data of **5**.

The first of these examined was the [3434]-4 conformation. Here the α-methylene protons were not in the same environment. One set occupied a corner position, while the other was on a 3-bond side. The H-2_{α} proton was deshielded by the anisotropy of the C-3–C-4 bond, while the H-2_{β} proton was deshielded by the anisotropy of the O–C-14 bond. These effects were of a similar magnitude, and a small $\Delta\delta$ value was predicted. In the case of the C-14 protons, the H-14_{exo} proton was deshielded by the anisotropy of the C-12–C-13 bond, but shielded by van der Waals steric interactions between H-14_{endo} and the H-3_{endo}, and H-11_{endo} protons calculated to be 2.18 and 2.23 Å away from H-14_{endo}. These van der Waals steric shielding effects opposed the larger anisotropic effect, and a smaller $\Delta\delta$ was expected than for the anisotropic shielding alone. The predicted line shape for these protons was more complex than observed here.

The β-methylene protons of the [3434]-4 conformation were expected to have a symmetric line shape as the result of anisotropy and van der Waals shielding effects. The H-3_{endo} proton was deshielded by the anisotropy of the C-2–O bond, and deshielded by a van der Waals steric repulsion with H-14_{endo}. The reverse effects were experienced by H-3_{exo}, and a mid-sized $\Delta\delta$ value was predicted. The H-13_{β} proton was deshielded by the anisotropy of both the C-11–C-12 bond and the O–C-14 bond. No van der Waals steric repulsions were expected since this proton occupied a corner position in this conformation. The anisotropy shielding effects were additive leading to a large $\Delta\delta$ value for C-13. Four signals were expected for the β-methylene protons in this conformation as a result of these effects with the signals of the C-3 protons flanked by the C-13 proton signals. However, the lowest field β-methylene proton signal at 1.86 ppm integrated to two-protons, where a one-proton signal at low-field for the H-13_{β} proton was expected for this conformation. The [3434]-4 conformation was therefore eliminated as a major conformation of **5**.

The non-diamond lattice [3344]-1 conformation was examined next. Here the distorted geometry placed the C-2 and C-14 protons in slightly different environments. The C-12 dihedral angle was calculated to be 16° less than in the [3434]-1 conformation resulting in a change to the anisotropic shielding of the C-14 protons. The calculated distances between the H-2_{endo} and H-5_{endo}, and the H-11_{endo} and H-14_{endo} protons were 2.27 and 2.29 Å, and small van der Waals steric repulsion contributions to the $\Delta\delta$ of the α-methylene protons were expected. The sum

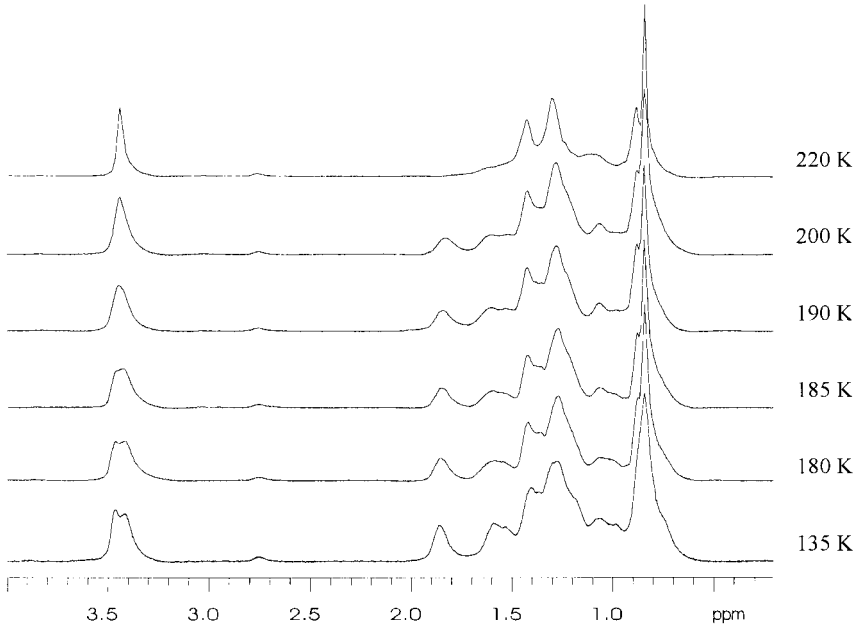

Figure 22. Variable temperature ^{1}H NMR (500 MHz) of ether **5**.

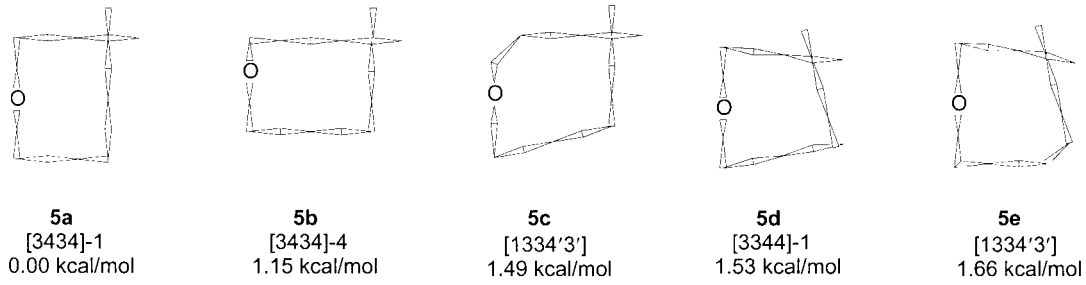

Figure 23. MM3* calculated low energy conformations of **5**.

of these effects could lead to four separate signals for the α-methylene protons. However, depending on the magnitude of the chemical shift changes caused by the dihedral angle distortion, the signals may be partially overlapped.

In the [3434]-1 conformation of **5**, the C-2 and C-14 protons adjacent to the ether oxygen were on a 4-bond side. The local environment of these methylenes was essentially equivalent, and any effects experienced by the C-2 protons were also experienced by the C-14 protons. The H-2_{exo} proton was deshielded by the anisotropy of the C-3–C-4 bond, and the H-2_{endo} proton was deshielded by a steric interaction with H-5_{endo}, calculated to be 2.22 Å away. This van der Waals steric repulsion resulted in a shielding of H-2_{exo} in opposition to the anisotropic shielding, and the magnitude of the overall shielding was reduced. The expected $\Delta\delta$ for the α-methylene protons in the [3434]-1 conformation was small in agreement with the DNMR spectra, and the [3434]-1 conformation is likely the major conformation of **5**. The downfield portion of the signal at 3.46 ppm was assigned to H-2_{exo} and H-14_{exo}, while the upfield portion at 3.42 ppm was assigned to the endo protons.

The C-3 and C-13 methylene protons in the [3434]-1 conformation were both located at corner positions, and similar chemical shifts for each methylene were expected. The H-3_{β} proton was deshielded by the anisotropy of both the C-4–C-5 bond, and the O–C-2 bond. These effects were additive and a large $\Delta\delta$ value was predicted. The relative integration of the β-methylene signals at 1.86, 1.59 and 1.52 ppm compared to the α-methylene signals at 3.4 ppm was approximately 2:1:1:4. The downfield signal at 1.86 ppm was assigned to H-3_{β} and H-13_{β}, while the upfield signals at 1.59 and 1.52 ppm were assigned to H-3_{α} and H-13_{α}. The chemical shift difference of the upfield signals at low temperature was approximately equal to the chemical shift difference of the C-3 and C-13 methylene protons at room temperature. It was unclear why this chemical shift difference was not also observed in the downfield signal. The DNMR data for the C-3 and C-13 protons of **5** were found to be consistent with the [3434]-1 conformation.

A ^{13}C DNMR study of **5** was carried out as well. One signal was observed for each of C-5, C-7 and C-6, the quaternary carbon, through the 145–220 K temperature range examined. The C-15 and C-16 geminal methyl carbons gave one signal at high temperature (220 K), a broad signal at 200 K, and two signals with a $\Delta\nu$ of 50 Hz as the temperature was lowered to 145 K. These results were consistent with a single conformation present at low temperature where the process of ring inversion was slow, and the C-15 and C-16 methyl group signals were no longer averaged.

A molecular mechanics search for low energy conformations of **5** was conducted using the Monte Carlo technique and the MM3* force field. The global minimum conformation was the [3434]-1 conformation **5a** with the [3434]-4 conformation **5b** calculated to have the next lowest energy, 1.15 kcal/mol higher. These calculations suggested the existence of four other low energy conformations within 2 kcal/mol of the global minimum conformation (Fig. 23). Higher energy conformations were ignored as they were not considered to be significantly populated. The relative population of these conformations at 135 K was calculated from the MM3* energies, and the [3434]-1 conformation **5a** was the major conformation (98%) in agreement with the DNMR data.

The transition state energies for the interconversion of conformations of **5** were determined from the DNMR spectra. The signals for the α-methylene protons had a $\Delta\nu$ of 21 Hz (T_c=190 K) while the β-methylene protons had $\Delta\nu$ values of approximately 149 Hz (estimated T_c=230 K). The $\Delta\nu$ for the C-15 and C-16 methyl signals in the ^{13}C DNMR study was 50 Hz (T_c=200 K) corresponding to a $\Delta G^{\ddagger}$ of 10.0±0.5 kcal/mol. The Dale interconversion mechanism transition state energies were calculated (MM3*) using the dihedral drive method with 10° increments of the dihedral angles. The energies of the [*1*3343] transition states for the interconversion of conformations **5a** and **5b** with **5d** were estimated at 10.7 and 10.4 kcal/mol (Fig. 24). The experimental and calculated transition state energies were in good agreement.

Macrocyclic ether **6** has a *gem*-dimethyl group at C-8. The room temperature ^{1}H NMR spectrum of ether **6** in $CDCl_3$ contained a four-proton triplet at 3.40 ppm for the C-2/C-14 protons, three four-proton multiplets between 1.53–1.58 ppm, 1.41–1.47 ppm and 1.28–1.35 ppm, an eight-proton multiplet between 1.14–1.24 ppm, and a six-proton singlet at 0.81 ppm for the C-8 geminal methyl groups. The ^{13}C NMR spectrum of **6** contained eight lines indicating that either **6** has a plane of symmetry, or is undergoing site exchange that is rapid on the NMR timescale. The ^{13}C signal downfield at 69.3 ppm was assigned to C-2/C-14, and the signal at 29.1 ppm was assigned to the C-8 geminal methyl groups. The signal at 32.8 ppm was of lesser intensity and was assigned to the quaternary C-8 carbon. The signal for

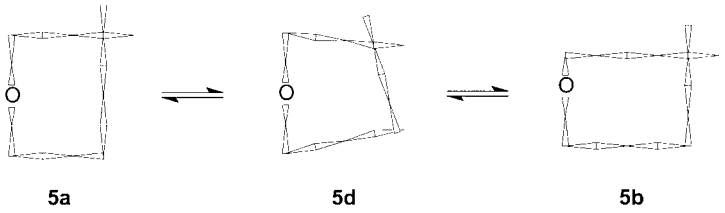

Figure 24. Interconversion of conformations of **5** via single corner movements.

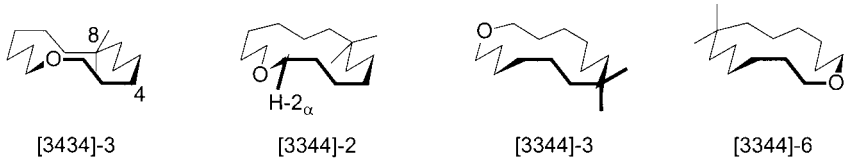

Figure 25.

carbons C-4/C-12 was shielded to 24.8 ppm, by a γ-gauche effect with the ether oxygen (Fig. 25).

The ^{1}H DNMR spectrum of **6** at 220 K contained six broad signals (Fig. 26). The downfield signal at 3.40 ppm for the C-2/C-14 protons broadened at intermediate temperatures then gave a pair of signals at 3.55 and 3.27 ppm as the temperature was lowered. The upfield signal at 3.27 ppm continued to broaden as the temperature was lowered further. The C-3 proton signal at 1.55 ppm broadened at temperatures below 185 K to give a downfield signal at 1.80 ppm, with another upfield signal presumably concealed by the methylene envelope. The C-8 geminal methyl group signal did not change significantly over the temperature range studied. This data was consistent with a single major conformation of **6** being present at low temperature.

It was significant that the signal for the C-8 geminal methyl groups remained averaged even at low temperature while the signal for the methylene protons adjacent to the ether oxygen did not. One possible explanation for this was that the major conformation of **6** was symmetric with a C_2 axis running through the C-8 corner atom. This C_2 axis would interconvert the equivalent C-8 geminal methyl groups. However, the protons adjacent to the ether oxygen would occupy inequivalent environments.

Low energy conformations of **6** must have the C-8 *gem*-dimethyl group at a corner position of the ring eliminating the [3434]-1 and [3434]-4 conformations, which would have transannular steric interactions involving an endo methyl group. The diamond lattice [3434]-3 conformation, and the non-diamond lattice [3344]-2, [3344]-3 and [3344]-6 conformations of **6**, where the C-8 *gem*-dimethyl group was located at a corner position were considered as possible low energy conformations of the macrocyclic ether **6**. With the exception of the [3344]-2 conformation, the ether oxygen atom was unfavorably located at a corner position

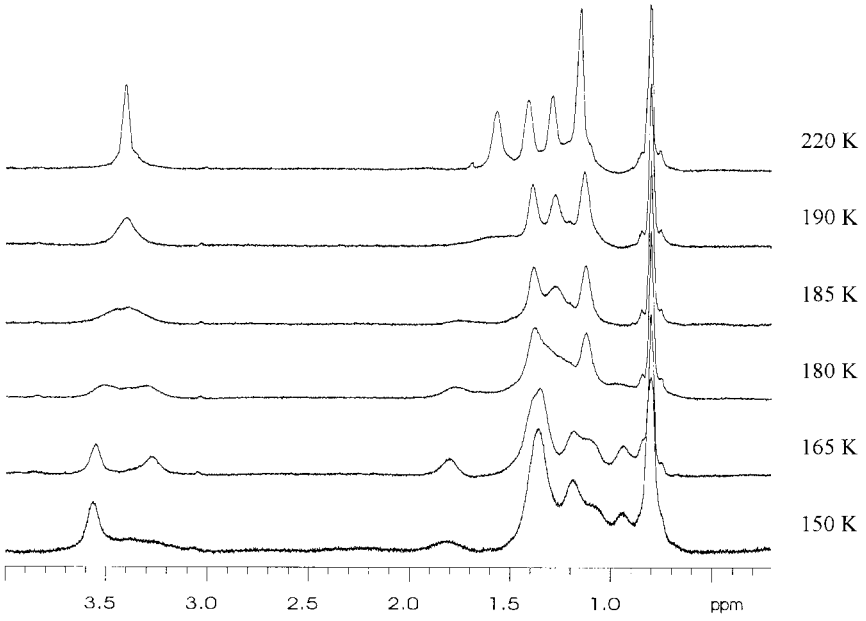

Figure 26. Variable temperature ^{1}H NMR (500 MHz) of ether **6**.

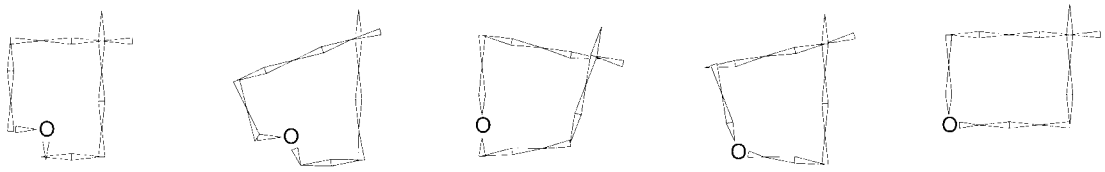

6a [22334] 0.00 kcal/mol | **6b** [22244] 0.41 kcal/mol | **6c** [3344]-2 0.68 kcal/mol | **6d** [3344]-6 1.61 kcal/mol | **6e** [3434]-3 1.97 kcal/mol

Figure 27. MM3* calculated low energy conformations of **6**.

in each of these conformations. In the [3344]-2 conformation some transannular hydrogen interactions would be eliminated by having the ether oxygen at a non-corner position, and this conformation was likely to have a low strain energy.

The two peaks observed in the DNMR spectra of **6** for the protons adjacent to the ether oxygen were of approximately equal intensity. In the [3344]-2 conformation, the C-2 corner protons would not experience any van der Waals steric interactions since both protons were exo to the ring. The H-2_{α} proton was deshielded by the anisotropy of the O–C-14 bond, but shielded by the anisotropy of the C-3–C-4 bond. These opposing effects were of a similar magnitude, and a small $\Delta\delta$ value was expected for the C-2 protons. The H-14_{endo} proton was deshielded by van der Waals steric interactions with the H-3_{epdo} and H-11_{endo} protons calculated to be 2.08 and 2.19 Å from H-14_{endo}. This resulted in a shielding of the H-14_{exo} proton, and a larger $\Delta\delta$ value than for the C-2 protons. In the [3434]-2 conformation, the line shape of the C-2 and C-14 protons was predicted to be more complex than that observed here in the DNMR spectra. The C-2 and C-14 protons were also in different environments in the diamond lattice [3434]-3 conformation where the line shape was predicted to be more complex than that observed here.

In the symmetric [3344]-3 and [3344]-6 conformations, the geometry of the C-2 and C-14 protons was similar in each conformation. The H-2_{exo} proton of the [3344]-3 conformation was deshielded by the anisotropy of the O–C-14 bond, but shielded by a van der Waals steric interaction between H-2_{endo} and H-13_{endo} calculated to be 2.12 Å apart. The predicted $\Delta\delta$ value for the H-2 protons in this conformation was small. The H-2_{exo} proton in the [3344]-6 conformation experienced both of these effects, and was further shielded by a van der Waals steric interaction between H-2_{endo} and H-5_{endo} calculated to be 2.18 Å apart. The $\Delta\delta$ between H-2_{endo} and H-2_{exo} in this latter conformation was predicted to be larger than that of the [3344]-3 conformation.

A molecular mechanics search for low energy conformations of **6** was conducted with the MM3* force field using the Monte Carlo technique. The global minimum conformation was found to be the non-diamond lattice conformation **6a** (Fig. 27). The second lowest energy conformation **6b**, was also a non-diamond lattice conformation, but symmetric and 0.41 kcal/mol higher in energy. The C-8 *gem*-dimethyl group was at a corner position in all of the low energy conformations. The first diamond lattice conformation found was **6e**, a [3434]-3 conformation with the ether oxygen at a corner position opposite to the C-8 *gem*-dimethyl group. Higher energy conformations were not considered to be significantly populated over the temperature range studied. The relative populations of these conformations at 150 K were calculated from enthalpy values ($\Delta H°$) and entropy values ($\Delta S°$) with both symmetry and mixing contributions, and the non-diamond lattice conformation **6a** was found to be the major conformation (81%) although conformations **6b** and **6c** were also calculated to have contributing populations of 10 and 8%, respectively.

The DNMR data of ether **6** was re-examined with the non-diamond lattice conformations **6a** and **6b** in mind. Conformation **6b** had a C_2 axis running through the C-8 corner position, and only one signal was expected for the geminal methyl groups. No transannular van der Waals shielding effects would be experienced by the C-2 and C-14 protons in these two conformations since they were all exo to the ring. The H-2_{β} and H-14_{α} protons were both deshielded by the anisotropy of the β-carbon–carbon bond in conformation **6a**, while the H-2_{β} and H-14_{β} protons were deshielded in conformation **6b**. The predicted $\Delta\delta$ values for the H-2 and H-14 protons in conformations **6a** and **6b** were consistent with the DNMR spectra. Overall, the DNMR data was consistent with either conformation **6b**, or with conformation **6a** where a local inversion to conformation **6b** could still occur at low temperature.

The transition state energies for the interconversion of conformations of **6** were calculated from the DNMR spectra. The C-2 proton signals had a $\Delta\nu$ of 139 Hz (T_c=190 K) corresponding to a $\Delta G^{\ddagger}$ of 8.8 kcal/mol. The energies of the Dale interconversion mechanism transition states were calculated (MM3*) with the dihedral drive method using a 10° increment.[25] The energies of the [*1*3343] transition state structures involved in the interconversion of the diamond lattice [3434]-3 conformation **6e** with the non-diamond lattice [3344]-2 and [3344]-6 conformations **6c** and **6d** were calculated at 13.4 and 14.2 kcal/mol, respectively (Fig. 28). These conformations are not interconvertable with the low energy conformations **6a** and **6b** via this mechanism. The low energy, non-diamond lattice conformations **6a** and **6b** can interconvert with each other via the Dale mechanism with an estimated transition state energy of 10.8 kcal/mol. This was in good agreement with the experimental value (DNMR) in support of the presence of these conformations.

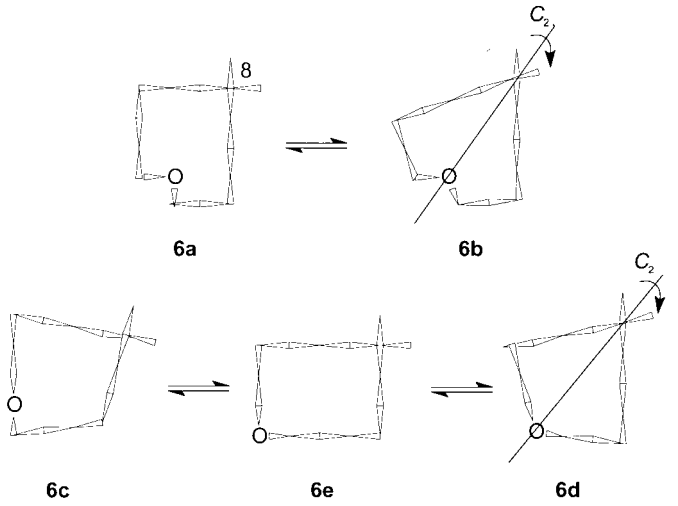

Figure 28. Interconversion of conformations of **6** via single corner movements.

Conclusion

The conformation of these 14-membered ethers was analyzed with data from ^{1}H DNMR experiments. The low-temperature chemical shift difference of protons with signals that were averaged at room temperature, were generally in agreement with predictions based on anisotropy and van der Waals shielding effects in the low energy conformations. Although many different possible conformations for these large ring compounds exist, only a few conformations were found to be appreciably populated at room temperature and below. The conformations were consistent with the substituents generally located exo to the ring, with geminal substituted carbon atoms occupying corner positions exclusively. These results were consistent with the molecular mechanics calculations. In general, the diamond lattice [3434] conformation was preferred with the oxygen atom at either the 1-position or the 4-position. Thus the introduction of the oxygen atom in these macrocyclic ethers did not have a significant effect on the conformation of the ring.

The transition state energies for the conformational interconversion of these ethers were determined from the ^{1}H DNMR experiments to be approximately 9–10 kcal/mol. The interconversion barriers of the C-2, C-3, and C-6 *gem*-dimethyl substituted macrocyclic ethers **3**–**5** were found to be higher than those of the other ethers studied. The calculated single corner movement transition state energies of the macrocyclic ethers were between 10 and 14 kcal/mol and higher than the observed values.

Experimental

The syntheses of these macrocyclic ethers have been previously reported.[3] Proton and carbon nuclear magnetic resonance spectra were recorded on deuteriochloroform solutions using a Bruker AMX-500 (^{1}H, 500 MHz, ^{13}C, 125 MHz) spectrometer. Chemical shifts are given in parts per million (ppm) on the δ scale, referenced to chloroform (δ 7.24 for ^{1}H and 77.0 for ^{13}C) as internal standard. Proton and carbon dynamic nuclear magnetic resonance spectra (DNMR) were recorded on Freon 21 ($CHCl_2F$) and Freon 22 ($CHClF_2$) (4:1) solutions using a Bruker AMX-500 spectrometer.

BATCHMIN, a part of the MACROMODEL molecular modeling program developed by Still and coworkers[27] was used to calculate the global minimum conformations of the macrocyclic ethers. A starting structure was chosen, random variations to internal coordinates were applied (torsional angles), the new structure was minimized using either the MM2* or the MM3* force field parameters, and the result was compared with conformations found during previous conformational search steps. After this resulting structure had been either stored as a new unique conformation or rejected as a duplicate, the cycle was repeated. This method is known as the Monte Carlo Multiple Minimum Search (MCMM). The MM2* and MM3* force fields are based on the MM2[28] and MM3[29] parameter sets developed by Allinger and coworkers.

Acknowledgements

We are grateful to the Natural Sciences and Engineering Research Council of Canada for financial support of this work. D. S. C. also thanks Dr T. V. RajanBabu for helpful suggestions regarding the preparation of this manuscript.

References

1. (a) Keller, T. H.; Neeland, E. G.; Rettig, S.; Trotter, J.; Weiler, L. *J. Am. Chem. Soc.* **1988**, *110*, 7858. (b) Keller, T. H.; Weiler, L. *J. Am. Chem. Soc.* **1990**, *112*, 450. (c) Neeland, E. G.; Ounsworth, J. P.; Sims, R. J.; Weiler, L. *J. Org. Chem.* **1994**, *59*, 7383. (d) Neeland, E. G.; Sharadendu, A.; Weiler, L. *Tetrahedron Lett.* **1996**, *37*, 5069.
2. Meyer, W. L.; Taylor, P. W.; Reed, S. A.; Leister, M. C.; Schneider, H.-J.; Schmidt, G.; Evans, F. E.; Levine, R. A. *J. Org. Chem.* **1992**, *57*, 291.
3. Clyne, D. S.; Weiler, L. *Tetrahedron* **1999**, *55*, 13659.

4. (a) Dale, J. *J. Chem. Soc.* **1963**, 93. (b) Dale, J. *Angew. Chem., Int. Ed. Engl.* **1966**, *5*, 1000.
5. Dale, J. *Acta Chem. Scand.* **1973**, *27*, 1115.
6. (a) Anet, F. A. L.; Cheng, K. *J. Am. Chem. Soc.* **1975**, *97*, 2420. (b) Anet, F. A. L.; Rawdah, T. N. *J. Am. Chem. Soc.* **1978**, *100*, 7810.
7. See Ref. 5 and Neeland, E.G. PhD Thesis, University of British Columbia, 1987.
8. Groth, P. *Acta Chem. Scand. A* **1976**, *30*, 155.
9. (a) Anet, F. A. L.; Cheng, A. K.; Wagner, J. J. *J. Am. Chem. Soc.* **1972**, *94*, 9250. (b) Drotloff, H.; Rotter, H.; Emeis, D.; Moeller, M. *J. Am. Chem. Soc.* **1987**, *109*, 7797.
10. Shannon, D. L.; Strauss, H. L.; Snyder, R. G.; Elliger, C. A.; Mattice, W. L. *J. Am. Chem. Soc.* **1989**, *89*, 1947.
11. Bassi, I. W.; Scordamaglia, R.; Fiore, L. *J Chem. Soc., Perkin Trans. 2* **1972**, 1726.
12. Groth, P. *Acta Chem. Scand. A* **1975**, *29*, 374.
13. Groth, P. *Acta Chem. Scand. A* **1979**, *33*, 503.
14. Dale, J. *Tetrahedron* **1974**, *30*, 1683.
15. ApSimon, J. W.; Craig, W. G.; Demarco, P. V.; Mathieson, D. W.; Saunders, L.; Whalley, W. B. *Tetrahedron* **1967**, *23*, 2339.
16. Cheney, B. V. *J. Am. Chem. Soc.* **1968**, *90*, 5386.
17. Bondi, A. *J. Phys. Chem.* **1964**, *68*, 441.
18. (a) Gschwendtner, W.; Schneider, H.-J. *J. Org. Chem.* **1980**, *45*, 3507. (b) Schneider, H.-J.; Buchheit, U.; Becker, N.; Schmidt, G.; Siehl, U. *J. Am. Chem. Soc.* **1985**, *107*, 7027.
19. Bovey, F. A.; Hood III, F. P.; Anderson, E. W.; Kornegay, R. L. *J. Chem. Phys.* **1964**, *41*, 2041.
20. Lambert, J. B.; Mixan, C. E.; Johnson, D. H. *J. Am. Chem. Soc.* **1973**, *95*, 4634.
21. Lambert, J. B.; Goldstein, J. E. *J. Am. Chem. Soc.* **1977**, *99*, 5689.
22. Friebolin, H. *Basic One- and Two-Dimensional NMR Spectroscopy*; VCH: New York, 1991, pp 263–272.
23. Anet, F. A. L.; Cheng, A. K.; Wagner, J. J. *J. Am. Chem. Soc.* **1972**, *94*, 9250.
24. Dale, J. *Acta Chem. Scand.* **1973**, *27*, 1130.
25. Wiberg, K. B.; Boyd, R. H. *J. Am. Chem. Soc.* **1972**, *94*, 8426.
26. Dale, J. *Top. Stereochem.* **1976**, *9*, 199.
27. Mohamadi, F.; Richards, N. G. J.; Guida, W. C.; Liskamp, R.; Lipton, M.; Caufield, C.; Chang, G.; Hendrickson, T.; Still, W. C. *J. Comput. Chem.* **1990**, *11*, 440.
28. Allinger, N. L. *J. Am. Chem. Soc.* **1977**, *99*, 8127.
29. Allinger, N. L.; Yuh, Y. H.; Lii, J.-H. *J. Am. Chem. Soc.* **1989**, *111*, 8551.